ELSEVIER

Tectonophysics 332 (2001) 309–320

TECTONOPHYSICS

www.elsevier.com/locate/tecto

Granular flow in polymineralic rocks bearing sheet silicates: new evidence from natural examples

M. Herwegh*, A. Jenni

Geological Institute, University of Berne, Switzerland

Received 4 April 2000; accepted 1 December 2000

Abstract

Natural deformation in carbonate mylonites bearing sheet silicates occurs via a complex interaction of granular flow and solution transfer processes and involves continuous cycles of dissolution, grain boundary diffusion, nucleation and growth. In this way, new sheet silicates (a) nucleate within voids formed by grain boundary sliding of calcite grains, (b) grow, and (c) rotate towards the shear plane. As a consequence, small mica grains show a wide range of orientations with respect to the shear plane, but moderate to large grains are subparallel both to each other and to the shear plane. Increases of average grain sizes with increasing temperature of sheet silicates in mica-rich layers is more pronounced than in mica-poor layers. In the calcitic matrix, however, sheet silicates can only grow via solution–precipitation and mass transfer processes. Therefore, the observed grain size variability indicates drastic differences in mass transfer behavior between the individual layers, which might be related to differences in the fluid flux. Based on these observations, a conceptual model for the microfabric evolution in sheet silicate bearing mylonites is presented.

Keywords: deformation mechanism; polymineralic rock; calcite; sheet silicate; Helvetics

1. Introduction

In naturally deformed rocks, sheet silicates are the predominant minerals that form foliation and white micas especially are very useful in dating of the deformation events (e.g. Hunziker et al., 1986; Huon et al., 1994 and references therein). Studies of the deformational behavior of sheet silicates reveal that rotation (March, 1932; Jeffrey, 1922), recrystallization (Marlow and Etheridge, 1977) or a combination of both (e.g. Oertel, 1983; Ishii, 1988; Ho et al., 1996) are the major foliation-forming processes. For the rotation of a crystal in non-coaxial flow three different models exist (e.g. Twiss and Moores, 1992): (a) rotation as a passive marker in the deforming rock (March model), (b) rotation as a rigid particle surrounded by a ductile matrix (Jeffrey model), or (c) the crystal can shear along its crystallographic shear planes and rotate towards the shear plane (Taylor–Bishop–Hill model). For the platy sheet silicates with their small thickness, the Taylor–Bishop–Hill model can be neglected. The Jeffrey model predicts a continuous rotation but elongated objects will rotate more slowly when they are parallel to the shear plane but rapidly when they are in orientations perpendicular to it. As a consequence of this model, sheet silicates should be found in all orientations but a concentration of orientations parallel to the shear plane is expected. Finally, rotation in terms of the March model would result in

* Corresponding author. Present address: Department of Earth, Atmospheric and Planetary Sciences, Massachusetts Institute of Technology, 77 Massachusetts Avenue, Cambridge, MA 02139, USA.

0040-1951/01/$ - see front matter
PII: S0040-1951(00)00288-2

sheet silicate orientations parallel to the shear plane from which the individual grains cannot rotate out anymore. Worley et al. (1997, p. 482) conclude that local advection combined with grain boundary diffusion is the dominant mass transport mechanism at lower greenschist facies metamorphic conditions but that volume diffusion is important at higher metamorphic grades.

In nature, however, sheet silicates are usually only one fraction among many and therefore their deformational behavior must be related to the deformation of matrix minerals. Silicate bearing carbonate mylonites are prominent natural examples and represent one of the most important mineral associations along thrust systems in the upper crust. Surprisingly, to our knowledge, no microstructural or experimental studies exist up to now that deal with the deformational behavior of this important polymineralic system. However, many rock deformation experiments performed on calcite show that, for aggregates consisting of small calcite grains, diffusion creep is the major deformation mechanism (e.g. Schmid et al., 1977; Walker et al., 1990). Additional processes including intracrystalline plasticity and grain boundary sliding are also required to be active to maintain strain compatibility (e.g. Schmid et al., 1977, 1987; Rutter et al., 1994). It is known that second-phase minerals can drastically influence both the microstructure and the rheology of a rock. Olgaard (1990), for example, presented a model in which pinning of the grain boundaries of the matrix mineral by second-phase particles can induce a change in the deformation mechanism. More recently, Herwegh and Kunze (submitted for publication) showed for carbonate mylonites that the ability of the microstructure to become refreshed by dynamic recrystallization is reduced with an enhanced content of organic nanoscale particles influencing both the calcite grain size and the texture. Therefore, an understanding of the interaction of deformation processes in the calcite matrix and sheet silicates is a crucial component of the rheological models for the upper crust and for isotopic dating of sheet silicates.

In this study, we use the sheet silicates in naturally deformed carbonate mylonites as a key to gain a better insight into the effect of deformation on the microstructure of this multicomponent system. The advantage of this system is that it contains only two rheologically significant phases that do not react. Based on the grain shape, size and orientation of the sheet silicates we are able to detect their deformational behavior in high-strain zones and discuss the role of diffusion in terms of variable sheet silicate content and temperature.

2. Sample material and analysis techniques

This paper focuses on samples of carbonate mylonites which derive from a N–S profile along the basal thrust of the Doldenhorn nappe (Central part of the Helvetic Alps, see Fig. 1). The thrust itself is between 1.5 and 5 m wide and has accommodated several kilometers of displacement, implying high strains within the shear zone. The emplacement of the Doldenhorn

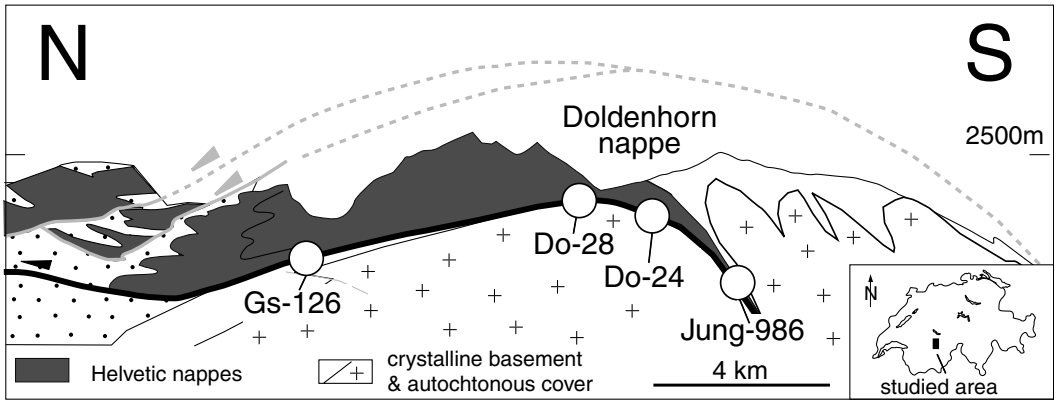

Fig. 1. N–S profile through the Helvetic nappe pile of Central Switzerland showing the sample locations along the basal thrust of the Doldenhorn nappe. Note that *T* increases from N to S.

Table 1
Modal compositions of sheet silicate bearing calcite mylonites

Sample	Sheet silicates	Dolomite and quartz	Calcite
Gs-126 rich	1.9	3.5	94.6
Do-28 rich	2.7	3.6	93.7
Do-24 rich	6.2	1.1	92.7
Jung986 rich	6.6	1.9	91.5
Gs-126 poor	0.02	0.23	99.75
Do-28 poor	0.3	0.5	99.2
Do-24 poor	0.6	0.6	98.8
Jung986 poor	0.1	0.2	99.7

nappe took place during a late stage of Alpine convergence (Kiental phase), just before the exhumation of the Helvetic nappe pile (Grindelwald phase, see Burkhard, 1988). Peak metamorphism in the area was lower greenschist facies and probably was contemporaneous with thrusting of the nappe (see Burkhard, 1988, 1993 and references therein). In general, the temperature increases in the studied area from North (340°C, Burkhard, 1990 to South $\approx$ 400°C).

In order to perform microstructural analyses, i.e. grain size and shape preferred orientations (SPO) of sheet silicates, rock chips of all samples were cut parallel to the nappe transport direction and perpendicular to the foliation. A two-step etching (Herwegh, 2000) resulted in partial dissolution of calcitic grains and their boundaries. Less-soluble second phases like sheet silicates, quartz, dolomite, pyrite and hematite (Table 1) form topographic peaks on the sample surface. Enhanced SEM acceleration voltages (20–30 keV) were used during digital imaging. Image analysis software allowed automatic segmentation of the individual grains of these second phases (Fig. 2). In most cases, the quality of the automatic segmentation had to be improved manually. Using the processed image, the volume proportions of second-phase minerals (Table 1), the lengths of their major and minor axes, and their orientations with respect to the foliation were calculated with NIH Image 1.61 (http://rsb.info.nih.gov/nih-image/). In the latter case, the angles between foliation and long axes are positive if anticlockwise measured and negative if

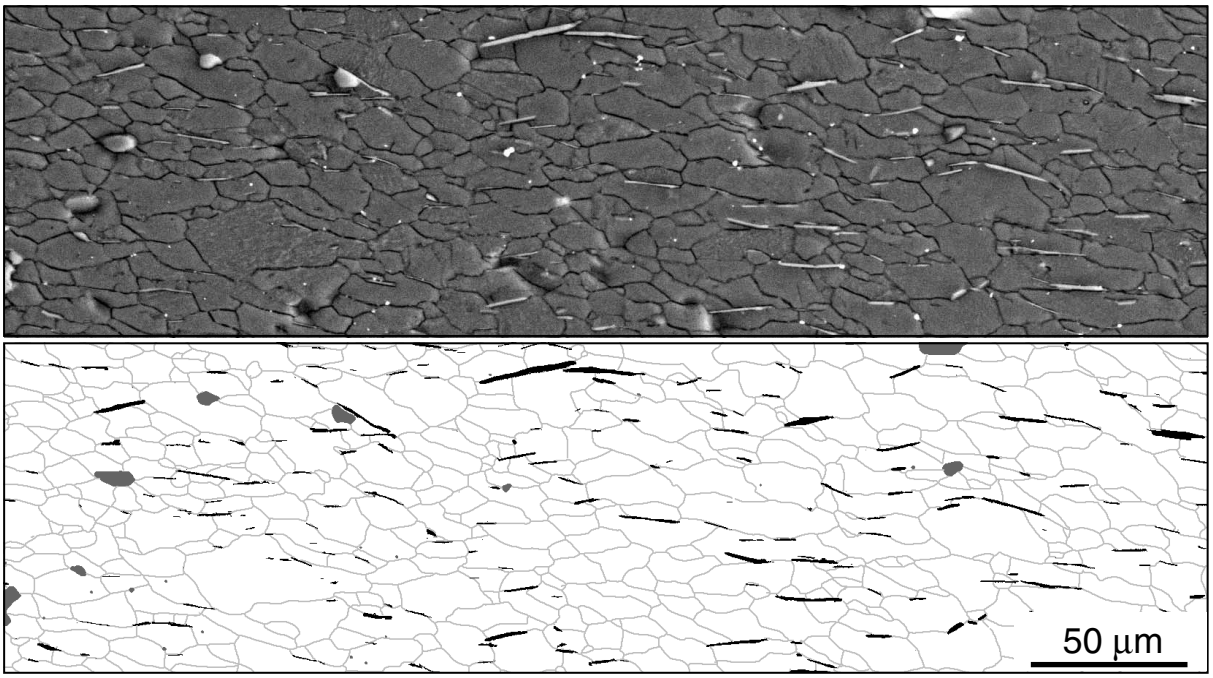

Fig. 2. Typical microstructure of a sheet silicate-rich layer with isolated sheet silicate grains embedded in the calcitic matrix (sample Do-28). (a) Backscatter electron image of the etched surface. (b) Resulting image after segmentation procedure: sheet silicates (black), calcitic matrix (white), and minor amounts of dolomite/quartz (gray).

clockwise measured for grains that are, respectively, narrower and more steeply inclined than the foliation. In order to discriminate the sheet silicates from other phases, only particles with axial ratios greater than 4:1 were used for the microstructural analysis. In addition, the size of dynamically recrystallized calcite grains of the pure layers was calculated by the method described by Herwegh (2000) for each sample.

Mineralogical compositions of the sheet silicates were analyzed by XRD on oriented samples with <2 and 2–16 μm size fractions (for technical details see Moore and Reynolds, 1985). Mixtures of muscovite and phengite were identified by applying the XRD technique described in Huon et al. (1994).

3. Results

SEM investigations reveal that the mylonites contain calcite layers with a variable mineral content of second phases, in particular sheet silicates. The original compositional banding, i.e. foliation, is subparallel to the major thrust plane. The calcite sheet silicate layers are several tens of microns thick. For this study, only those layers were selected for analysis in which (a) the individual sheet silicate grains were embedded in a calcitic matrix and (b) no shear bands exist (Fig. 2). We distinguish between two general types of layer with varying calcite/sheet silicate content (Table 1), henceforth referred to as 'sheet silicate-rich' and 'sheet silicate-poor' layers. At this point it is important to note that even in the case of the sheet silicate-rich layers, the content of sheet silicates is smaller than 7 vol% (Table 1). Besides sheet silicates, quartz and dolomite exist in subordinate amounts while feldspar, hematite and pyrite can occur as accessories. XRD analyses suggest that most sheet silicates are two-phase micas (muscovite, phengite, see also Huon et al., 1994), but small amounts of chlorite and muscovite–chlorite mixed layers are also present.

The sheet silicates occur preferentially along the calcite grain boundaries (Fig. 3). Considerable variation in the shape of individual sheet silicate grains allows us to distinguish three general types (Fig. 3). Type A sheet silicates are typical platelet-like grains with high axial ratios and straight grain boundaries (Fig. 3a). Type B grains are represented by tiny sheet silicate grains with straight grain boundaries. They usually sit along triple junctions of calcite grains and the individual grains often show sudden changes in their thickness (Fig. 3b). Type C grains are sheet silicates with curved grain boundaries, irregular shapes, and lower axial ratios (Fig. 3c–e). Many of these sheet silicate grains appear to be bent (compare Fig. 3c and d).

Both the range and mean values of the long axes increase from N to S in the tectonic profile, changing from 30 to 150 and from 5 to 20 μm, respectively, in sheet silicate-rich layers (Table 2, Figs. 4 and 5). A similar increase in grain size is observed in the calcitic matrix where the average major axes of grains range from 18 to 50 μm. Furthermore, calcite grains have straight grain boundaries and elongated shapes (Figs. 2 and 3).

The results of several hundreds of sheet silicate

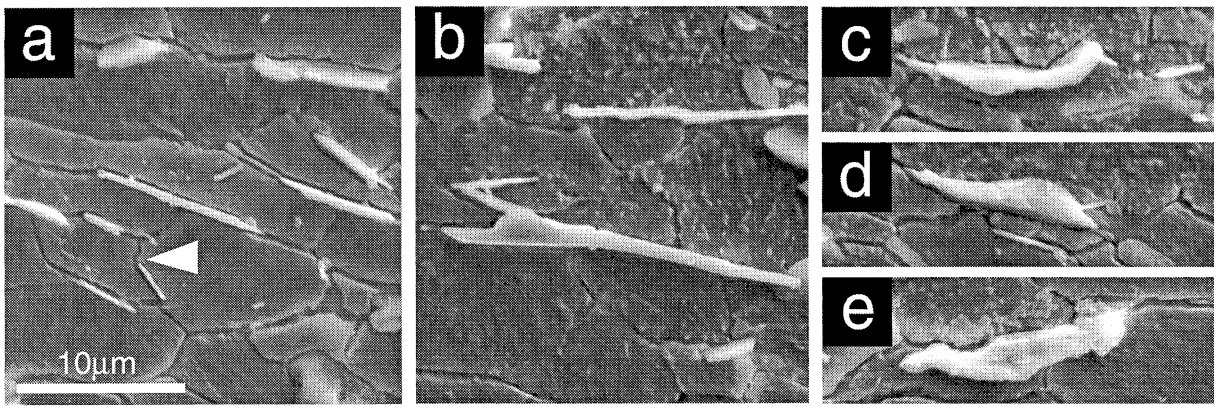

Fig. 3. Typical grain morphologies of: (a) Type A, (b) Type B and (c–e) Type C sheet silicate grains. See text for explanation.

orientations from sheet silicate-rich layers are presented in Fig. 5. In this figure the orientation of the major axes with respect to the shear plane is shown as a function of grain size. In a first step, the number of grains per class have been counted using class sizes of 2 and 4 μm/10°, respectively, for samples Do-24 to Do-28 and sample Jung-986. In a second step, a contouring was performed on these counts using contour intervals of 1, 2, 4, 6, 8–15, 16–31 and ≥32 grains. Fig. 5 renders two important observations: (a) The shear plane parallel foliation is defined by a compositional banding which mainly results from variations in the sheet silicate content between the individual layers. Interestingly, both the major axis of sheet silicate and calcite grains within the individual layers are slightly oblique with respect to the sample-scale foliation (~10–15°). Note that this geometric relationship is in excellent agreement with the orientation of intergranular microshears observed in simple shear experiments of rock analogues (see Herwegh and Handy, 1998). (b) Short sheet silicates are much more scattered in orientation; there is a broad spread of angles in the range from −50 up to 60°. This spread continuously decreases with increasing sheet silicate length ending in an angular range of about 25° for the biggest grains. Interestingly, the center point (cross in Fig. 5) of the highest contour interval and therefore also the range of big angular spread, shifts towards bigger grain sizes with increasing temperature (Fig. 5). Furthermore, the number of grains inclined at positive angles with respect to the foliation is bigger than that of those with negative inclinations (Fig. 5). Note that few grains are oriented perpendicular to the foliation. The March model as the most commonly used model to describe the evolution of platy minerals in shear zones predicts that all sheet silicate grains should end with their major axes parallel to the shear plane, a prediction in contrast to the distributions found in our samples even though all samples have seen very high shear strains.

Fig. 6 compares grain size of sheet silicates from poor and rich regions with those of calcite grains from sheet silicate-poor areas, i.e. calcite grains that are unaffected by second-phase minerals (data from Table 2). This comparison suggests that calcite and sheet silicate grain size correlate. In other words, the sheet silicates can grow with increasing temperature although isolated and embedded in a calcitic matrix. However, Fig. 6 indicates that over the entire temperature range (a) the calcite grain sizes increase more than those of the sheet silicates and (b) the grain coarsening of sheet silicates is more intense in silicate-rich parts.

4. Deformation related processes: discussion

4.1. Rotation of sheet silicates

In all samples, sheet silicates are embedded in a calcitic matrix (Fig. 2) and therefore have to interact with this matrix during deformation. One possible interaction is the rotation of the sheet silicate platelets as rigid objects in a viscous matrix (March, 1932; Jeffrey, 1922). In fact, this rotational behavior is indirectly manifested by the orientation of sheet silicates with intermediate to large grain sizes. These grains have major axes subparallel to each other within a small orientational range of about 25° (see Fig. 5). The slight obliquity of the long axis of both calcite and sheet silicate grains with respect to the foliation (10–15°, see Figs. 2 and 5), i.e. the shear plane, could be related to intergranular microshear zones and the

Table 2
Lengths of sheet silicate and calcite grains

Sample	Sheet silicate-rich layers		Sheet silicate-poor layers		Calcite	
	Sheet silicate length	Grains	Sheet silicate length	Grains	Calcite major axis	Grains
GS-126	5.2 ± 3.6	350	5.5 ± 2.4	5	18.4 ± 13.2	682
Do-28	6.7 ± 4.7	706	7.4 ± 4.4	11	18.2 ± 16.3	429
Do-24	9.7 ± 8.2	380	7.1 ± 5.9	79	26.0 ± 21.9	433
Jung-986	15.7 ± 14.5	693	7.9 ± 3.9	48	50.0 ± 35.0	349

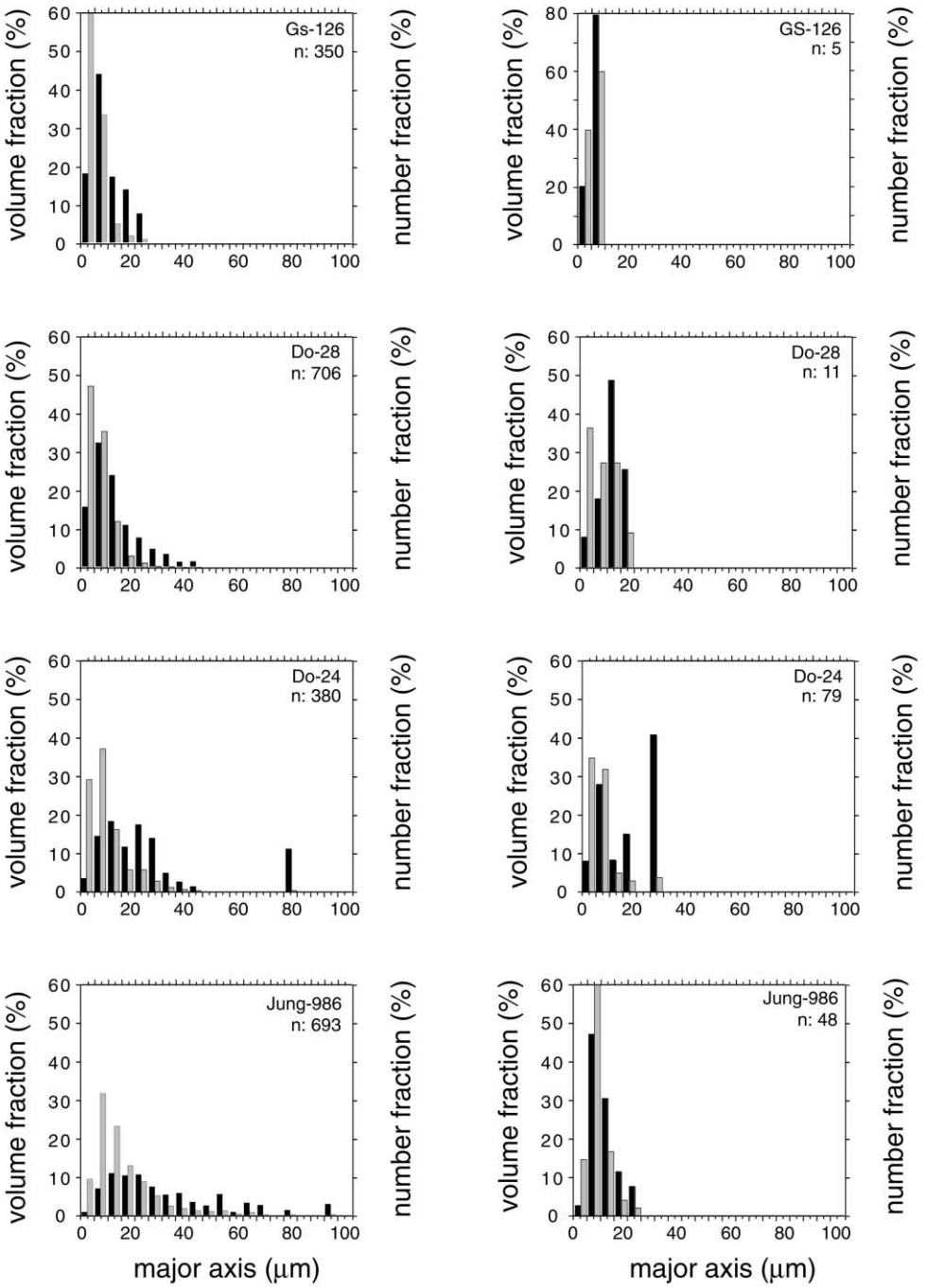

Fig. 4. Volume (black) and number weighted (gray) histograms for the major axes of sheet silicate grains for sheet silicate-rich (left column) and -poor (right column) layers. Increasing *T* from top to bottom, *n*: number of sheet silicate grains analyzed.

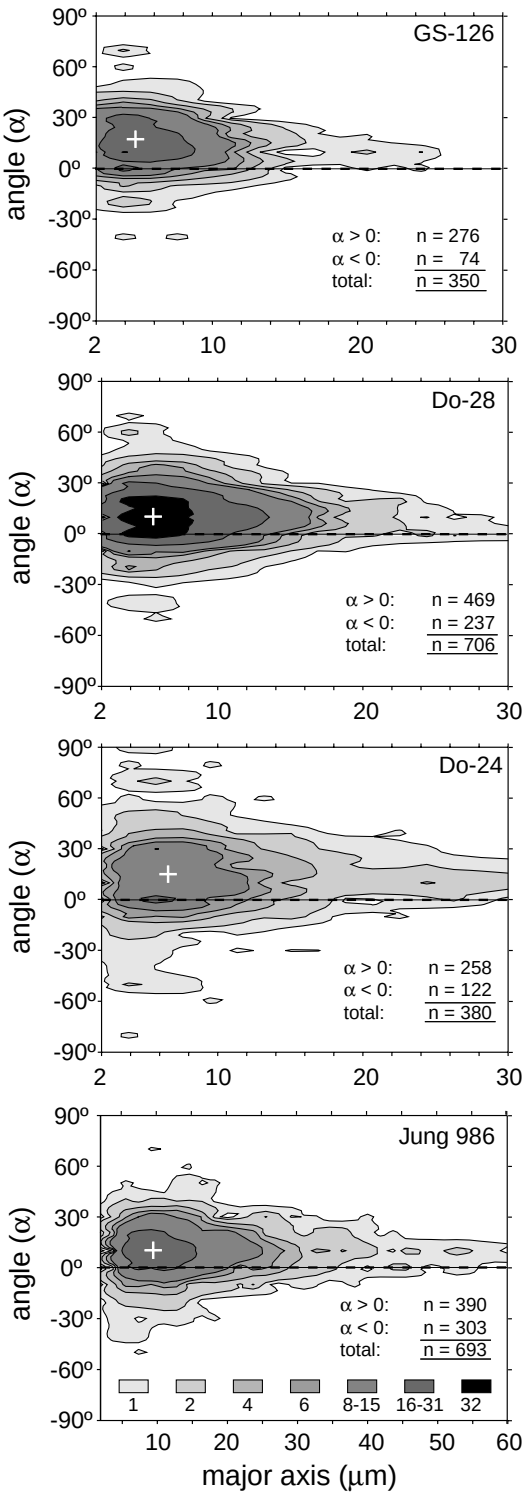

Fig. 5. Diagrams show the relationship between the orientation (angle α) and the length of the major axis of sheet silicates. Contour intervals give the number of sheet silicates within each class (i.e. 1, 2, 4, 6, 8–15, 16–31, ≥32 grains). *n*: number of sheet silicates, increasing *T* from top to bottom.

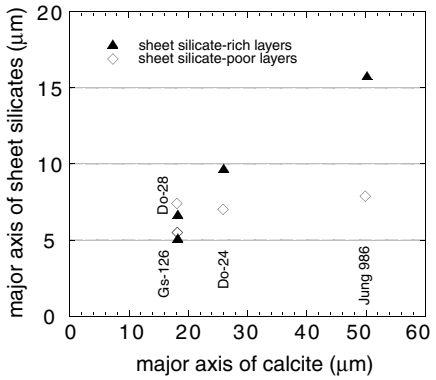

Fig. 6. Variations of length of sheet silicates as a function of the length of recrystallized calcite grains. Note that the calcite measurements derive from silicate-poor layers with only limited influence of second phases on the calcite grain sizes.

associated resetting behavior of calcite grains (see also Herwegh and Handy, 1998). Detailed studies on the spatial relationship of the sheet silicates could eventually be used to identify former microshear zones which cannot be resolved anymore from the microstructure of the matrix minerals (see also Herwegh and Handy, 1998; Bons and Jessell, 1999). Such studies are important to understand the localization and distribution of strain in polyphase aggregates.

In contrast, the broad orientational scatter of small-sized sheet silicates that continuously decreases with increasing grain size (see Fig. 5) can definitely not be explained by a simple March type rotation although all sheet silicate grains within a specimen (a) derive from a high-strain shear zone, (b) are located in the same kinematic framework, (c) co-exist at the same temperature, and (d) have high axial ratios (<4:1). Also, the Jeffrey model fails because in this case not only the small-sized but all sheet silicate grain size fractions should represent at least some grains at high-angle orientations with respect to the shear plane. The most plausible way out of this discrepancy between model and observation is to postulate different relative ages for the individual grains requiring additional

processes like diffusive mass transport, continuous nucleation and growth of grains.

4.2. Diffusive mass transfer

The assumption of diffusive mass transfer of sheet silicates in a calcitic matrix is critical because of higher solubilities of calcite in water under low-T conditions than those of sheet silicates (e.g. Oertel, 1983) implying a high efficiency for calcite dissolution–precipitation processes. Nevertheless, the following arguments indicate the existence of diffusional processes in the samples analyzed: the sheet silicate coarsened with increasing temperature (Figs. 4 and 5), which is in agreement with studies on phyllosilicates (Ishii, 1988). However, in our samples the sheet silicates are isolated and simple coarsening by grain boundary migration can be excluded. Mass transfer in complete solid state as an alternative is not efficient enough because it is too slow under these low-temperature conditions (see Worley et al., 1997). Therefore, grain coarsening of sheet silicates must be associated with mass transfer along grain boundaries between source regions to sink regions (see Paterson, 1995). The sources may be of Type C grains; their irregular shapes and grain boundaries may reflect dissolution phenomena along silicate–calcite interfaces (Fig. 3c–d). The sinks may be the idiomorphic and unbent Type A grains (Fig. 3a). Type A grains are located generally along the boundaries of calcite grains and may indicate that grain boundary diffusion is the dominant mechanism.

4.3. The control of diffusive mass transfer

The matrix grain size can be used to indicate the integrated temperature history of the rock. Larger matrix sizes indicate longer times and higher temperature. Even though the temperature at a certain time within a single sample is constant, Fig. 6 shows that, for a given matrix grain size, the sheet silicates grain size in mica-rich layers (5–7 vol%) increases more rapidly than in poor layers ($<$1.2 vol.%). If the grain size increase is principally due to Ostwald ripening (see e.g. Eberl et al., 1990), then smaller intergranular transport distances from sources to sinks in combination with an enhanced availability of appropriate ions in sheet silicate-rich parts may cause the rapid coarsening.

Mass transfer is most efficient in the presence of a fluid phase (Paterson, 1995). The existence of fluids during deformation in the basal thrust of the Doldenhorn nappe is confirmed by the occurrence of synkinematic calcite veins. However, the fact that sheet silicate-rich and -poor layers are only a few microns thick and are intercalated with each other implies that: (a) fluid compositions during deformation must have had large chemical gradients between the different layers; (b) no homogenization between the different fluid layers took place; and (c) the source sink distances for solution mass transfer must have been small at least in directions perpendicular to the shear plane (20–30 μm). We assume that nucleation and growth are not rate-limiting because this would require both a similar number of new grains and an identical grain size distribution in sheet silicate-poor and -rich layers. Mass transfer must therefore have occurred in the fluid by diffusion along grain boundaries. Fluid convection as an alternative mass transfer process can be excluded because in this case a homogenization between the different layers would be expected.

Thus calcite–sheet silicate interfaces may therefore be more favorable for intergranular mass transfer than calcite–calcite grain boundaries resulting in localized material pathways within the polymineralic parts of the carbonate mylonite. These assumptions nicely confirm previous studies (e.g. Chamberlain and Conrad, 1991; Ferry, 1988), which showed that variations in mineral content control the rate of diffusion in different layers. As discovered recently by Farver and Yund, 1999), rocks rich in sheet silicates are characterized by enhanced geochemical transport and exchange rates which can be up to 4 orders of magnitude faster than in monomineralic rocks. Besides differences in diffusion rates between different layers, diffusion rates parallel to the foliation of mica bearing rock types can be up to two to ten times faster than those perpendicular to it (Farver and Yund, 1999).

4.4. Nucleation and growth of sheet silicates

The combination of small grain size, broad orientational scatter and fresh idiomorphic grain shape suggests that the small-sized sheet silicates must be nucleated. In terms of nucleation, temperatures are constant on the sample scale and can be excluded as

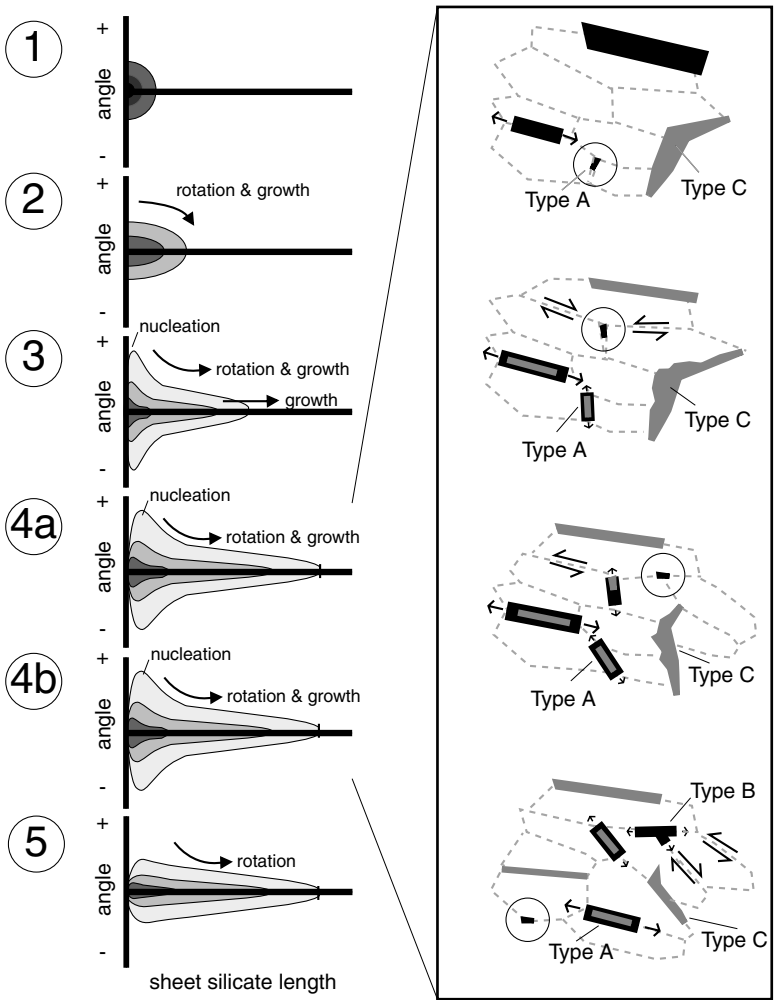

Fig. 7. Conceptual model of the evolution of a sheet silicate bearing mylonite. First column shows the changes of sheet silicate orientation and length with time: (1) sedimentation, (2) diagenesis and incipient metamorphism, (3) onset of ductile deformation, (4) steady state deformation, and (5) final stages of ductile deformation. The inset presents schematically the changes in size, orientation and shape for Type A, B and C sheet silicates.

a potential driving force. Alternatively, local variations in pore pressure and fluid chemistry can induce nucleation processes. For example, the opening of voids induced by grain boundary sliding of calcite grains leads to the infiltration of local grain boundary fluids and can lower the local fluid pressure. As a consequence, the fluid becomes oversaturated with the appropriate ions favoring heterogeneous nucleation. The morphology of the Type B grains is consistent with nucleation in voids which were induced by grain boundary sliding (see also Ree, 1994). Note that this deformation sequence is similar to the model of vein formation suggested by Etheridge et al. (1984), except that in our carbonate mylonites, the processes occur on the grain scale instead of larger scale convections and grain boundary sliding creates dilatancy instead of fracturing. Apparently local mass transfer controls the source–sink behavior.

The broad orientational range of the small-sized sheet silicates implies that their nucleation orientations are arbitrary, and that they depend more on local strain incompatibilities than on preferred orientations with

respect to the bulk kinematic framework. Although the nucleation of sheet silicates is controlled by the calcite matrix (i.e. calcite grain size), the sheet silicates themselves can control the calcite microstructure by dragging and pinning the calcite grain boundaries (see white arrow in Fig. 3a and Olgaard and Evans, 1988; Olgaard, 1990) or by influencing the locations of source–sink sites in calcite aggregates during solution mass transfer via grain boundary sliding.

At this point it is important to note that in spite of the vorticity of non-coaxial flow, few small-sized Type A grains survived at very high angles with respect to the shear plane. Therefore these sheet silicates must have been formed immediately before the microfabric became frozen in, i.e. during the very last stages of ductile deformation.

5. A conceptual model

Based on the aforementioned observations, we present in this section a conceptual model for the evolution of a sheet silicate bearing mylonite. Assuming a random distribution of clay flocs in a calcitic micrite after sedimentation (1 in Fig. 7), rotation and growth of the sheet silicates combine to induce a first foliation during soft sediment compaction and diagenesis (2 in Fig. 7, see also Oertel, 1983).

With increasing metamorphic grade, the calcite matrix deforms by a combination of grain boundary sliding, intracrystalline plasticity and solution transfer processes and a steady state is approached (3 and 4 in Fig. 7). In the sheet silicates, (a) old deformed Type C grains become dissolved, (b) mass transfer occurs along the grain boundaries in the polymineralic aggregate, (c) new grains nucleate in random orientations along grain boundary voids of the calcite matrix (e.g. small Type A grains and Type B grains), and (d) grains grow and rotate towards the shear plane (big Type A grains). All these processes occur simultaneously and can be found within the same specimen (inset in Fig. 7). Continuous nucleation results in the broad orientational scatter of small-sized sheet silicates while the rotational component is manifest by the parallelism of intermediate to large-sized grains (3–4b in Fig. 7).

With increasing temperatures, the average steady state grain sizes of both newly nucleated and rotated grains increases (4a and b in Fig. 7). In addition to temperature, the steady state grain size of the sheet silicates is affected by the fraction of sheet silicates per unit volume, i.e. the availability of appropriate ions and the transport distances between sources and sinks. Thus, a higher flux of ions per volume induces bigger sizes of sheet silicate grains in sheet silicate-rich layers. (Fig. 6). Owing to limited fluid exchange between individual layers, original compositional differences between the different layers (i.e. perpendicular to the foliation) can persist to very high shear strains.

On the retrograde path, rapid exhumation of the shear zone without any further shearing will preserve the steady state microfabric (4a and b in Fig. 7) while continuous shear deformation and a decrease in temperature will reduce the mass transfer and the ability of sheet silicates to nucleate. Under the assumption of viscous deformation of the calcitic matrix, in the latter case, all sheet silicates will tend to rotate towards the shear plane (5 in Fig. 7) and the steady state character of the microstructure will be destroyed.

6. Conclusions and implications

Sheet silicate bearing rocks belong to the most important rock types of the upper crust. This study shows that the deformation of such polymineralic systems involves a close interaction between deformation processes in both the calcite matrix and the second-phase minerals, i.e. sheet silicates. In order to describe upper crustal rheology, the use of end-member flow laws could be misleading because they do not incorporate the interactions of deformation processes between the minerals.

In comparison to Means (1981) and Herwegh and Handy (1998) the associated steady state microfabric is dynamically preserved by continuous dissolution, diffusive mass transfer, nucleation, growth, and rotation (Fig. 7) and can therefore best be described by granular flow combined with solution transfer processes (compare with Paterson, 1995). In the light of rheological models, however, rock deformation experiments on polymineralic carbonate mylonites are required to obtain well-defined databases.

With respect to K–Ar dating of white micas, the model presented above explains why even in the finest

grain size fraction, old detrital signatures can at least partially persist (compare with Huon et al., 1994) as a consequence of incomplete dissolution. For future studies we therefore recommend the following: (a) Use only samples which have seen high shear strains, i.e. samples from thrust contacts, because they most probably are equilibrated chemically by the aforementioned cycles of formation and destruction. (b) In the case of variable sheet silicate content, focus first on sheet silicate-rich layers because they are closer to chemical equilibrium. (c) Perform selected analyses with the laser ablation method on individual sheet silicate grains in dependence of their size and orientation. Such an approach could give new insights into the chemical exchange behavior during deformation and the absolute timing of thrusting events.

Acknowledgements

G. Rizzoli kindly helped us with the XRD analysis of the sheet silicates. The stimulating discussions with A. Berger, R. Heilbronner, M. Jessell and H. Stünitz helped to significantly improve the present study. A. Berger and B. Evans are gratefully acknowledged for reviewing an earlier version of this manuscript. Finally, we would like to thank the two journals referees, D. Bruhn and H.-R. Wenk, for their constructive reviews.

References

Bons, P.D., Jessell, M.W., 1999. Micro-shear zones in experimentally deformed octachloropropane. J. Struct. Geol. 21, 332–334.

Burkhard, M., 1988. L'Helvetique de la bordure occidentale du massif de l'Aar (évolution tectonique et métamorphique). Eclogae Geol. Helv. 81, 63–114.

Burkhard, M., 1990. Ductile deformation mechanisms in micritic limestones naturally deformed at low temperatures (150–350°C). In: Knipe, R.J., Rutter, E.H. (Eds.), Deformation Mechanisms, Rheology and Tectonics. Geological Society Special Publication, vol. 54, pp. 241–257.

Burkhard, M., 1993. Calcite twins, their geometry, appearence and significance as stress–strain markers and indicators of tectonic regime: a review. J. Struct. Geol. 15, 351–369.

Chamberlain, C.P., Conrad, M.E., 1991. The relative permeabilities of quartzites and schists during active metamorphism at mid-crustal levels. Geophys. Res. Lett. 18, 959–962.

Eberl, D.D., Sordon, J., Kralik, M., Taylor, B.E., Zell, E.P., 1990. Ostwald ripening of clays and metamorphic minerals. Science 248, 413–520.

Etheridge, M.A., Wall, J.H., Cox, S.F., 1984. High fluid pressures during metamorphism and deformation: implications for mass transport and deformation mechanisms. J. Geophys. Res. 89, 4344–4358.

Farver, J.R., Yund, R.A., 1999. Oxygen bulk diffusion measurements and TEM characterization of a natural ultramylonite: implications for fluid transport in mica-bearing rocks. J. Metamorph. Geol. 17, 669–683.

Ferry, J., 1988. Contrasting mechanisms of fluid flow through adjacent stratigraphic units during regional metamorphism, south-central Maine, USA. Contrib. Mineral. Petrol. 98, 1–12.

Herwegh, M., 2000. A new technique to automatically quantify microstructures of fine grained carbonate mylonites: two step etching combined with SEM imaging and image analysis. J. Struct. Geol. 22, 391–400.

Herwegh, M., Handy, M.R., 1998. The origin of shape preferred orientation in mylonite: inferences from in-situ experiments on polycrystalline norcamphor. J. Struct. Geol. 20, 681–694.

Herwegh, M., Kunze, K., submitted for publication.

Ho, N.-C., Peacor, D.R., Van der Pluijm, B.A., 1996. Contrasting roles of detrital and authigenic phyllosilicates during slaty cleavage development. J. Struct. Geol. 18, 615–623.

Hunziker, J.-C., Frey, M., Clauer, N., Dallmeyer, R.D., Friedrichsen, H., Flehmig, W., Hochstrasser, K., Roggwiler, P., Schwander, H., 1986. The evolution of illite to muscovite: mineralogical and isotopic data from the Glarus Alps, Switzerland. Contrib. Mineral. Petrol. 92, 157–180.

Huon, S., Burkhard, M., Hunziker, J.-C., 1994. Mineralogical, K–Ar, stable and Sr isotope systematics of K-white micas during very low-grade metamorphism of limestones (Helvetic nappes, western Switzerland). Chem. Geol. 113, 347–376.

Ishii, K., 1988. Grain growth and re-orientation of phyllosilicate minerals during the development of slaty cleavage in the South Kitakami Mountains, northeast Japan. J. Struct. Geol. 10, 145–154.

Jeffrey, G., 1922. The motion of ellipsoidal particles immersed in a viscous fluid. Proc. R. Soc. Lond. A 102, 161–179.

March, A., 1932. Mathematische Theorie der Regelung nach der Korngestalt bei affiner Deformation. Z. Kristallogr. 81, 285–297.

Marlow, P.C., Etheridge, M.A., 1977. Development of layered crenulation cleavage in mica schists of the Kanmantoo Group near Macclesfield, South Australia. Bull. Geol. Soc. Am. 88, 873–882.

Means, W.D., 1981. The concept of steady-state foliation. Tectonophysics 78, 179–199.

Moore, D.M., Reynolds, R.C., 1985. X-ray Diffraction and the Identification and Analysis of Clay Minerals. Oxford University Press, Oxford, 326 pp.

Oertel, G., 1983. The relationship of strain and preferred orientation of phyllosilicate grains in rocks — a review. Tectonophysics 100, 413–447.

Olgaard, D.L., 1990. The role of second phase in localizing deformation. In: Knipe, R.J., Rutter, E.H. (Eds.), Deformation Mechanisms, Rheology and Tectonics. Geological Society Special Publication, vol. 54, pp. 175–181.

Olgaard, D.L., Evans, B., 1988. Grain growth in synthetic marbles with added mica and water. Contrib. Mineral. Petrol. 100, 246–260.

Paterson, M.S., 1995. A theory for granular flow accommodated by material transfer via an intergranular fluid. Tectonophysics 245, 135–151.

Ree, J.H., 1994. Grain boundary sliding and development of grain boundary openings in experimentally deformed octachloropropane. J. Struct. Geol. 16, 403–418.

Rutter, E., Casey, M., Burlini, L., 1994. Preferred crystalplastic orientation development during the plastic and superplastic flow of calcite rocks. J. Struct. Geol. 16, 1431–1446.

Schmid, S.M., Paterson, M.S., Boland, J.N., 1977. Superplastic flow in fine-grained limestone. Tectonophysics 43, 257–291.

Schmid, S.M., Panozzo, R., Bauer, S., 1987. Simple shear experiments on calcite rocks: rheology and microfabric. J. Struct. Geol. 9, 747–778.

Twiss, R.J., Moores, E.M., 1992. Structural Geology. Freeman, New York, 532 pp.

Walker, A.N., Rutter, E.H., Brodie, K.H., 1990. Experimental study of grain-size sensitive flow of synthetic, hot pressed calcite rocks. In: Knipe, R.J., Rutter, E.H. (Eds.), Deformation Mechanisms, Rheology and Tectonics. Geological Society Special Publication, vol. 54, pp. 259–284.

Worley, B., Powell, R., Wilson, C.J.L., 1997. Crenulation cleavage formation: evolving diffusion, deformation and equilibration mechanisms with increasing metamorphic grade. J. Struct. Geol. 19, 1121–1135.